Turkish Journal of Electrical Engineering & Computer Sciences

http://journals.tubitak.gov.tr/elektrik/

Research Article

Turk J Elec Eng & Comp Sci
(2021) 29: 2154 – 2169
© TÜBİTAK
doi:10.3906/elk-2009-126

A hybrid technique using modified ICP algorithm for faster and automatic 2D & 3D microscopic image stitching in cytopathologic examination

Hülya DOĞAN[1,*], Elif BAYKAL KABLAN[1], Murat EKİNCİ[1], Mustafa Emre ERCİN[2], Şafak ERSÖZ[2]

[1]Department of Computer Engineering, Faculty of Engineering, Karadeniz Technical University, Trabzon, Turkey
[2]Department of Pathology, Faculty of Medicine, Karadeniz Technical University, Trabzon, Turkey

Received: 18.09.2020 • **Accepted/Published Online:** 20.05.2021 • **Final Version:** 26.07.2021

Abstract: Due to the limitations of the light microscopic system such as limited depth of field and narrow field of view, entire sample areas are invisible and pathologists move the light microscope stage along the X - Y - Z axes with eye-hand coordination. In order to reduce the dependence on the pathologist and to allow whole sample areas to be examined in a short time without any control (without eye-hand coordination), this study creates 2D & 3D panoramic images with wide-view of sample in the light microscopic systems. According to our literature research, there is no study that creates 2D & 3D panoramic images in the microscopic system together. For this reason, it is thought that our study, which is the first one in which 2D & 3D panoramic images are created together in the light microscopic system, will be one of the pioneering studies in this field. Literature studies generally utilize specific microscope types such as laser, stereo and confocal, where 3D shape of the sample is extracted automatically and only 2D & 3D microscopic image stitching techniques are performed. Unlike these studies, due to the use of the light microscope which is requires a procedure to extract the 3D structure of the sample, this study contains an extra phase which creates 2D & 3D adjacent images using series of multi-focus 2D adjacent images before 2D & 3D microscopic image stitching technique. Moreover, a hybrid 2D & 3D microscopic image stitching technique which uses modified ıterative closest point algorithm and combines the stages of 2D and 3D image-based 2D & 3D image stitching techniques is developed in this study. Both qualitative and quantitative evaluations of the proposed study are performed on real microscope image data sets from samples prepared for cytopathologic examination in the light microscopic system. Our hybrid technique creates 2D panoramic images whose values of peak signal to noise ratio (PSNR), correlation coefficient (CC), entropy and average gradient are computed respectively as 30.4267, 0.9997, 7.4670 and 122.2510 and 3D panoramic images whose values of PSNR, universal quality index, root mean square error, CC, kurtosis metric and standard deviation are computed respectively as 17.7458, 0.9702, 8.9230, 0.8702, 5.4981 and 31.006, which are the best values when compared with well-established studies. Moreover, the proposed hybrid technique with 9.8403 and 23.5902 (s) execution times accelerates the process of automatic 2D & 3D panoramic imaging.

Key words: Modified iterative closest point, cytopathologic examination, automatic 2D & 3D microscopic image stitching, speeded up robust features, light microscopic system, 2D & 3D panoramic imaging

1. Introduction

During cytopathologic examination, pathologists use a light microscopic system to observe the structure of the cells in the sample taken from patient. Some partial areas of the sample are seen in the cytopathologic

*Correspondence: hulya@ktu.edu.tr

This work is licensed under a Creative Commons Attribution 4.0 International License.

examination due to restrictions in the light microscopic system, such as narrow field of view and limited depth of field. In order to analyze all areas on the sample, pathologist is required to move the stage of light microscope along the X - Y - Z axes with eye-hand coordination. Dependence on the pathologist's experience is very time consuming and can lead to incorrect treatment and symptoms in diagnosing the disease. Automatic 2D & 3D microscopic image stitching provides ultra-high resolution panoramic imaging. Therefore, the pathologist can investigate 2D & 3D panoramic images with whole sample areas in a short time without any control (without eye-hand coordination). Moreover, diseases can be diagnosed more accurately in 2D & 3D panoramic images, where the positions and size of the cells are more realistic, and the structure of the cells is more pronounced.

Since 2D & 3D image stitching is one of the most popular topics in the research fields including medical imaging, computer vision, remote sensing and computer graphics, literature techniques have been actively developed over the years. These techniques can be divided into two different groups: 2D image-based and 3D image-based, schematic diagrams of which are shown in Figure 1. The main stages (pairwise registration and image and height fusion) of these techniques are similar. Unlike 2D image-based techniques, 3D adjacent images (3D source and reference images) are used in 3D image-based techniques to calculate a transformation matrix. The pairwise registration stages of two groups allow the alignment of 2D & 3D source images to the coordinate system of 2D & 3D reference images by using the transformation matrices, whose sizes are 3 x 3 for 2D image-based and 4 x 4 for 3D image-based stitching techniques. In classical pairwise registration, two basic operations are implemented: (1) course registration, where a rough initial alignment between 2D & 3D source and reference images is provided, and (2) fine registration, where 2D & 3D source images are transformed into the coordinate system of 2D & 3D reference images by calculating a transformation matrix. In the coarse registration operations of two groups, firstly, feature points are extracted in the source and reference images. Harris corner detection algorithm, scale ınvariant feature transform (SIFT) and speeded up robust features (SURF) are methods used in 2D image-based techniques to extract feature points in 2D adjacent images. For 3D image-based techniques, feature points of 3D adjacent images are extracted using three different algorithms based on greedy search, global and local features. Literature studies report that the methods used to match the feature points of adjacent images in 2D image-based and 3D image-based stitching techniques are different. 3D image-based stitching techniques generally utilize Brute force matching or K-d trees nearest neighbor search algorithm, while cross-correlation or Euclidean distance is used in 2D image-based stitching techniques. In the fine registration of 2D image-based stitching techniques, random sample consensus (RANSAC) is implemented to minimize matching errors and to predict the model that defines the relationship between 2D & 3D adjacent images. Similarly, the most commonly used algorithm for the fine registration of 3D image-based stitching techniques is ıterative closest point (ICP). In image and height fusion stages of two groups, 2D & 3D panoramic images are created by calculating the pixel values and heights of overlapping areas in the 2D & 3D adjacent images.

Although automatic 2D & 3D microscopic image stitching is one of the most researched areas in the microscopic systems, there is no study in which 2D & 3D panoramic images with a wide-view sample in the microscopic system are created together according to our literature research. Therefore, the literature approaches recommended for the creation of panoramic images with a wide-view sample in the microscopic system are explained by two different titles as 2D microscopic image stitching and 3D microscopic image stitching in this study. (1) 2D microscopic ımage stitching approaches: Literature studies related to 2D microscopic image stitching can be classified as follows: (i) Improving the efficiency of 2D panoramic image with a wide-view of the sample in the microscopic system, where a new pre-processing stage or algorithm was proposed to crate the

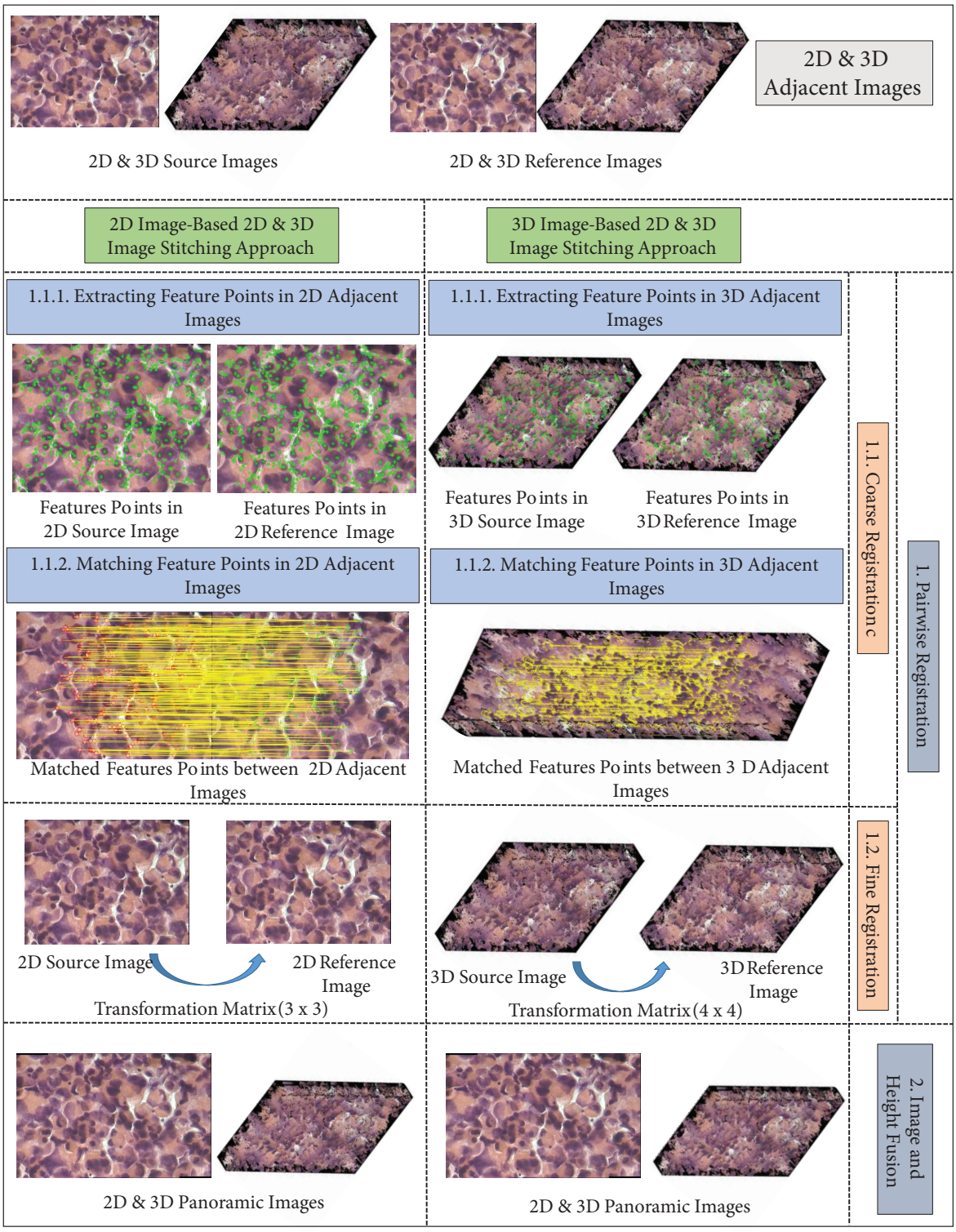

Figure 1. Schematic diagrams of 2D image-based and 3D image-based 2D & 3D image stitching techniques: (1) Pairwise registration, (2) Image and height fusion.

2D panoramic image with less noisy and seamless overlapping areas [1–11]. (ii) Accelerate the 2D microscopic image stitching system, where researchers developed a tool or algorithm to provide more accurate and rapid 2D panoramic imaging with a wide-view of the sample [12–16]. (iii) Real-time realization of 2D microscopic image stitching system [17–19]. (2) 3D microscopic ımage stitching approaches: Similar to 2D microscopic image stitching, literature approaches related to 3D microscopic image stitching have been improved for many years. These approaches generally presented a framework or tool that can be used to create a 3D panoramic image with a wide-view of the sample in the microscopic system. Examples for these tools are as follows: XuvTools [20], globally optimal stitching [21], TeraStitcher [22], microscopy image stitching tool (MIST) [23], high-resolution ımage stitching [24], logical stitching [25], BigStitcher [26], ThingiPano [27] and Miniscope3D [28]. For these approaches, researchers prepared large 3D microscopic databases using specific types of the microscopes, which are laser, stereo and confocal. Furthermore, no procedure is needed to extract the 3D structure of the samples in these specific microscope types.

The primary objective of our study is to suggest a novel approach for faster and automatic 2D & 3D microscopic image stitching in cytopathologic examination. Contrary to literature studies, 2D & 3D panoramic images with a wide-view of the sample in the light microscopic system can be created together in the proposed approach. It comprises two main phases: (i) creating 2D & 3D adjacent ımages and (ii) hybrid 2D & 3D microscopic ımage stitching technique. The first phase creates 2D & 3D adjacent images using the series of multi-focus 2D adjacent images. In the second phase, a hybrid 2D & 3D microscopic image stitching technique, which combines the stages of 2D image-based and 3D image-based 2D & 3D image stitching techniques, is developed. This phase contains two main stages: (1) pairwise registration, where classical Iterative closest point algorithm is modified to align 2D & 3D source images to the coordinate system of 2D & 3D reference images and (2) image and height fusion that produces 2D & 3D panoramic images with a wide-view of the sample by calculating the pixel values and heights of overlapping areas in the 2D & 3D the adjacent images. The achievement of the suggested technique is tested on real microscope images data sets from samples prepared for cytopathologic examination in the light microscopic system. The effectiveness of the proposed technique is compared with well-known studies by utilizing performance assessment metrics with and without requiring a 2D or 3D ground-truth panoramic image. It is proven that the suggested technique produces more accurate 2D & 3D panoramic images in less time than other existing techniques.

2. Methodology

As shown in Figure 2, this study purposes to produce 2D & 3D panoramic images with a wide-view of the sample in the light microscopic system, and generates two main phases which are creating 2D & 3D adjacent ımages and hybrid 2D & 3D microscopic ımage stitching technique.

2.1. Creating 2D & 3D adjacent images

Series of multi-focus adjacent images are used to create 2D & 3D adjacent images. In this phases, firstly, a series of multi-focus reference images are generated by moving the microscope stage with a step motor along the specific distance, which is randomly defined between the start and end locations on the Z axis. Then, the microscope stage is moved along the X or Y axes, and a series of multi-focus source images are generated by scanning the same distance of multi-focus reference images. 2D adjacent images are determined by auto-focusing algorithm. ın the auto-focusing algorithm, a focus value for each multi-focus image in the series is calculated by using auto-focus function, and a 2D image with the highest focus value is selected from the series. 3D adjacent

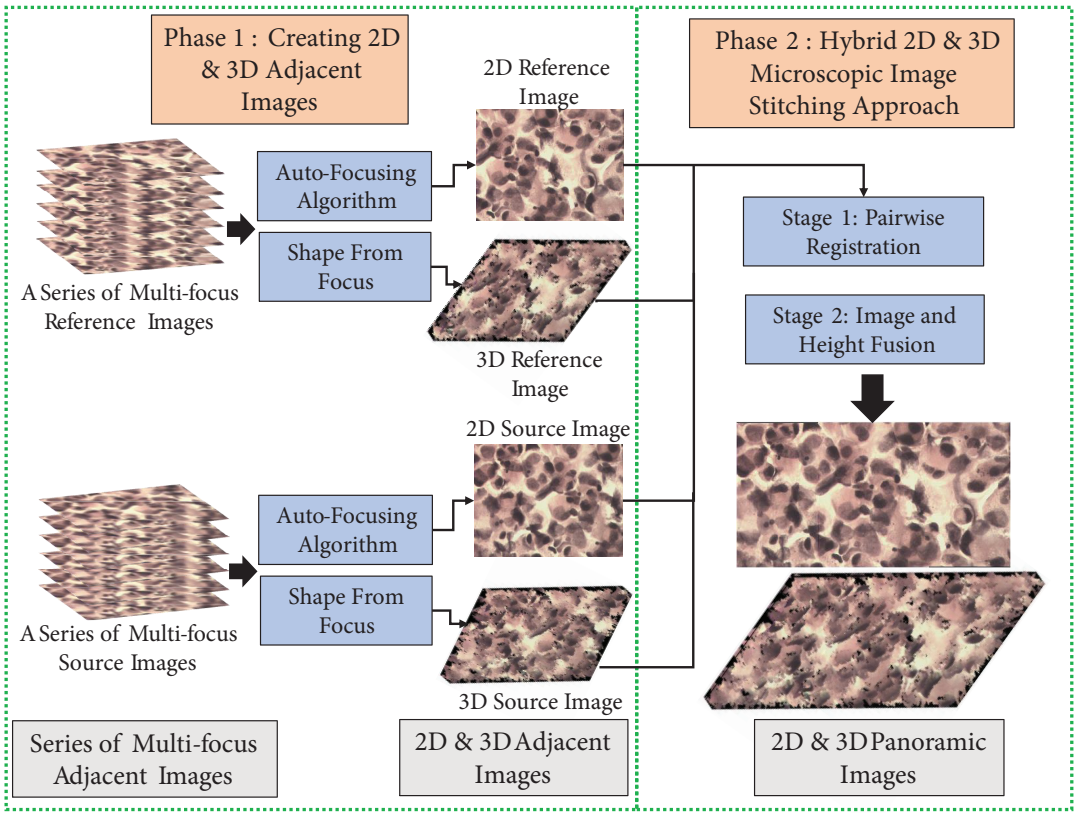

Figure 2. Schematic diagram of two main phases applied to produce 2D & 3D panoramic images with a wide-view of the sample in this study: (i) Creating 2D & 3D adjacent ımages, and (ii) Hybrid 2D & 3D microscopic ımage stitching technique.

images are created with Shape From Focus, which is a strategy that generates a 3D structure using the series of 2D multi-focus images. The steps performed in the designed shape from focus strategy are given in Figure 3 and summarized as follows: (1) RGB components of 2D multi-focus images $(MFI_1, MFI_2, ..., MFI_N)$ are converted to YCbCr color components, where N refers to the indices of the 2D multi-focus images. (2) Y components of 2D multi-focus images are taken as focus values of pixels, and a series of focus values for 2D multi-focus images $(FV_1, FV_2, ..., FV_N)$ are created. (3) Focus value vectors $(FV_{x,y} = FV_1(x, y), FV_2(x, y), ..., FV_N(x, y))$ are formed for all pixel coordinates of 2D multi-focus images, where x and y indicate the pixel coordinates in the 2D multi-focus images. (4) 3D image is estimated by searching the highest pixel focus value on the focus value vectors.

2.2. Hybrid 2D & 3D microscopic image stitching technique

2D & 3D panoramic images with a wide-view of the sample in the light microscopic system are created together using 2D & 3D adjacent images produced in previous phases. In this phase, a hybrid 2D & 3D microscopic image stitching technique, which combines the stages of 2D image-based and 3D image-based 2D & 3D image stitching techniques is developed. As seen in Figure 4, the presented 2D & 3D microscopic image stitching technique is performed in two fundamental stages, which are pairwise registration and ımage and height fusion.

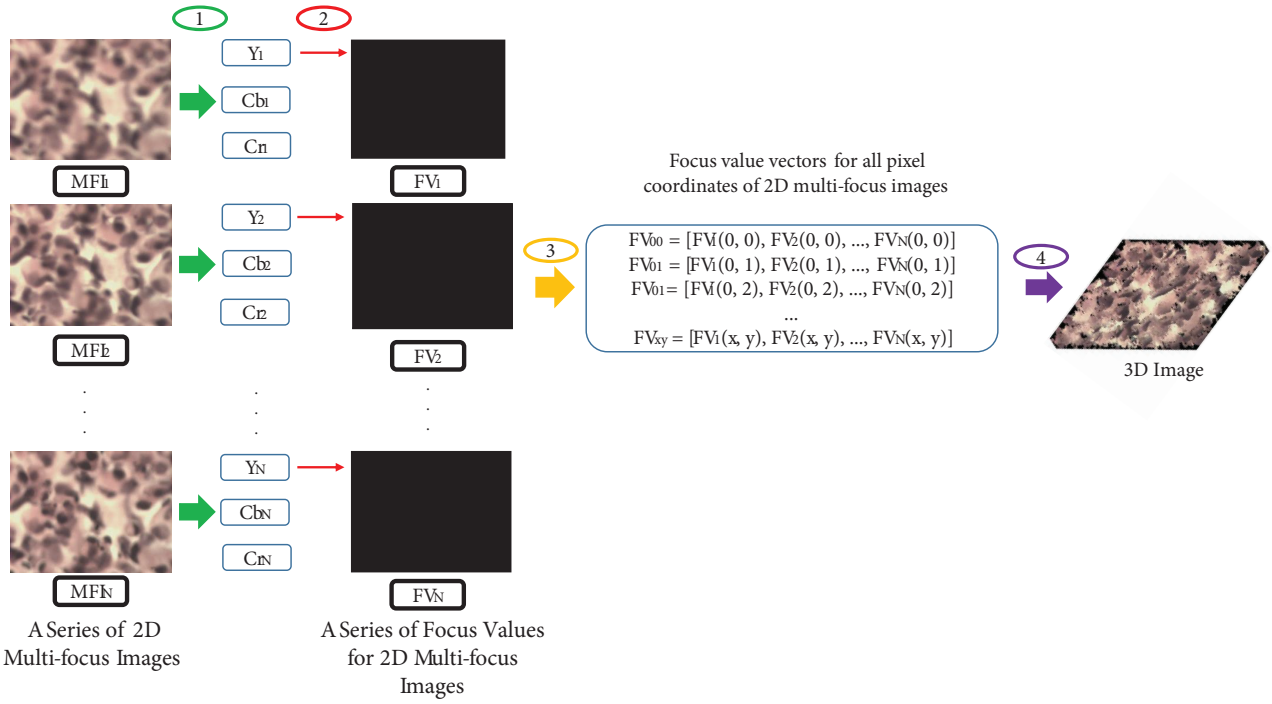

Figure 3. The steps performed in shape from focus strategy.

2.2.1. Pairwise registration

Pairwise registration aligns 2D & 3D source images to the coordinate system of 2D & 3D reference images using 2D adjacent images (2D source and reference images). For faster and more accurate 2D & 3D panoramic imaging, classical ıterative closest point algorithm is modified in this study. The steps performed in modified ıterative closest point algorithm are summarized as follows:

1. Extracting feature points in 2D adjacent ımages: In the first step of modified ıterative closest point algorithm, feature points in 2D source and reference images are extracted. To reduce the proposed technique complexity, the feature points ($\overrightarrow{c_s} = [s_1, s_2, s_3, .., s_n] - \overrightarrow{c_r} = [r_1, r_2, r_3, .., r_m]$) in 2D source and reference images are selected using SURF algorithm.

2. Matching feature points in 2D adjacent ımages: The feature points extracted with SURF algorithm in the 2D source ($\overrightarrow{c_s} = [s_1, s_2, s_3, .., s_n]$) and reference ($\overrightarrow{c_r} = [r_1, r_2, r_3, .., r_m]$) images are matched using K-d trees nearest neighbor search algorithm. In this step, firstly, k-dimensional tree structure of feature points in the 2D reference image is generated. Then, the closest neighbor point for each point in the 2D source image is selected from this tree structure.

3. Projecting the matched feature points in 2D adjacent images to 3D adjacent images: To determine the matched feature points in the 3D source and reference images, the matched feature points in the 2D adjacent images are projected to the 3D adjacent images using reflection method.

4. Computing transformation matrix between 3D adjacent images: For the alignment of 2D & 3D source images to the coordinate system of 2D & 3D reference images, this step computes the transformation

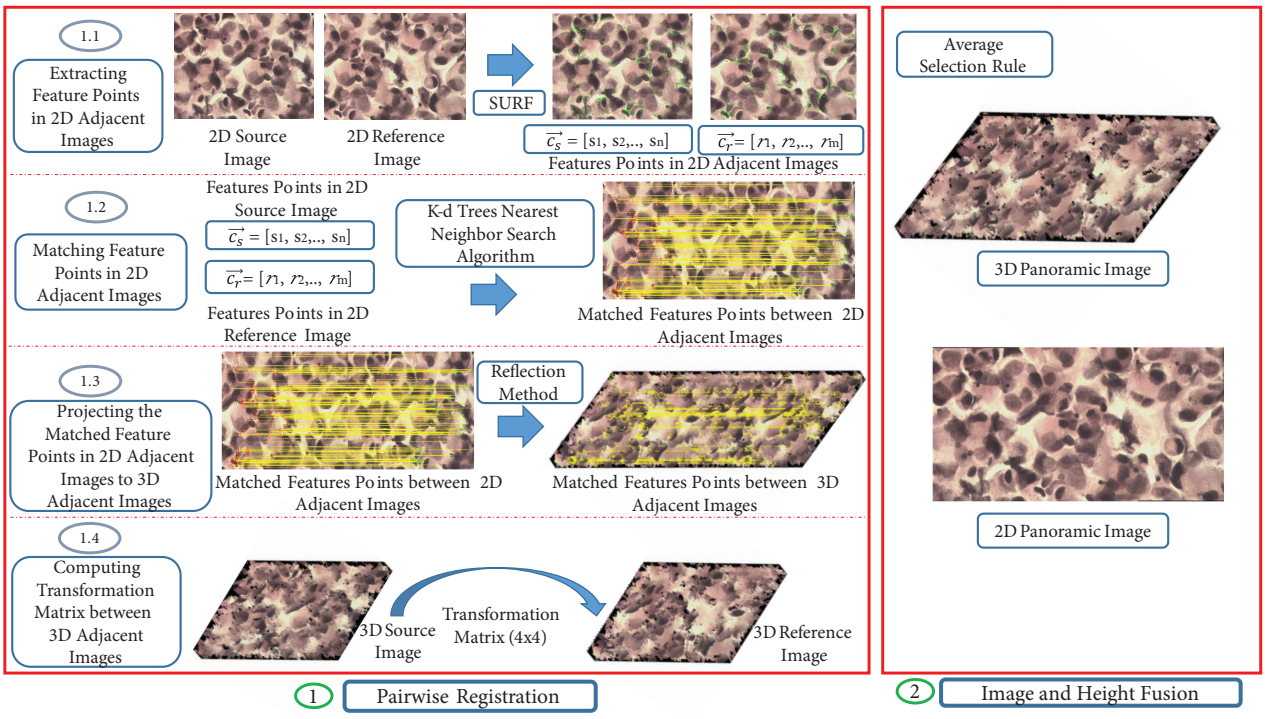

Figure 4. Schematic diagram of two main stages applied into hybrid 2D & 3D microscopic image stitching technique: (i) pairwise registration and (ii) ımage and height fusion.

matrix (4x4) between the 3D source and reference images. The operations performed in this step are as follows:

(a) Centers of 3D source ($\overrightarrow{m_s}$) and reference ($\overrightarrow{m_r}$) images are computed as seen in (1).

$$\overrightarrow{m_s} = \frac{1}{N}\sum_{i=1}^{N}\overrightarrow{s_i} \qquad \overrightarrow{m_r} = \frac{1}{N}\sum_{i=1}^{N}\overrightarrow{r_i} \tag{1}$$

where $\overrightarrow{s}$ and $\overrightarrow{r}$ denote the matched feature points between the 3D source and reference images, N is the number of the matched feature points.

(b) The centers of 3D source and reference images are re-centered by calculating covariance matrix (H) as shown in (2).

$$H = \sum_{i=1}^{N}(\overrightarrow{s_i} - \overrightarrow{m_s})(\overrightarrow{r_i} - \overrightarrow{m_r})^T \tag{2}$$

(c) Rotation (R) matrix is computed using singular value decomposition (SVD) as given in (3).

$$[U, S, V] = SVD(H) \qquad R = VU^T \tag{3}$$

(d) Translation vector ($\overrightarrow{t}$) is computed as seen in (4).

$$\overrightarrow{t} = -R * \overrightarrow{m_s} * \overrightarrow{m_r} \tag{4}$$

(e) Transformation matrix ($T - 4x4$) in (5) is obtained by combining the rotation matrix ($R - 3x3$) with the translation vector ($\overrightarrow{t} - 3x1$).

$$R = \begin{bmatrix} a & d & g \\ b & e & h \\ c & f & i \end{bmatrix} \qquad \overrightarrow{t} = \begin{bmatrix} k & l & m \end{bmatrix} \qquad T = \begin{bmatrix} a & d & g & k \\ b & e & h & l \\ c & f & i & m \\ 0 & 0 & 0 & 1 \end{bmatrix} \tag{5}$$

3D source image is transformed to the coordinate system of 3D reference image with the transformation matrix (T). The error between the transformed 3D source image and 3D reference image is calculated using (6).

$$Error = \sum_{i=1}^{N} T * \overrightarrow{s_i} - \overrightarrow{r_i} \tag{6}$$

The error between the transformed 3D source image and 3D reference image is compared with a threshold value. Previous steps continue until the error is less than the threshold value.

2.2.2. Image and height fusion

Average selection rule is applied in the image and height fusion stage to calculate the pixel values and heights of overlapping areas in the 2D and 3D panoramic images.

3. Experiments and discussion

3.1. Device configuration and data sets

A device configuration is used for the implementation of the proposed approach, which consists of Matlab 2018B running on a PC with Intel Core i7-9750 and 2.60 GHz processor, 16 GB RAM and NVIDIA GeForce RTX 2060 GPU. The 2D & 3D microscopic image stitching techniques used in the study are performed with our own codes in Matlab environment, and its special functions are used to show visually the results of 3D panoramic images. Moreover, a novel motorized light microscope system is established in this study, which can scan on the sample along the X - Y - Z axes automatically. It is used to acquire real microscopic image data sets for the analysis of the proposed 2D & 3D microscopic image stitching technique. Our novel motorized system contains several materials: a light microscope, a monitor, a PC with Intel Core i7 CPU, 8 GB RAM and Windows 10 operating system, three step motors, which are used to move the microscope stage along the X - Y - Z axes, a digital microscope CCD camera, a step motor control circuit which provides data transfer between three step motors and PC.

In order to assess our proposed technique more objectively, different data sets, which consist of real microscope images are created. Microscopic image data sets and properties are outlined in Table 1. Two different samples are scanned to acquire the images in the data sets. These samples are prepared for Pathology

Laboratory's cytopathological examination at Medicine Faculty in Karadeniz Technical University, Trabzon, Turkey. The light microscopic systems do not contain any 2D or 3D ground-truth panoramic images. In order to produce 2D and 3D ground-truth panoramic images, which are used for performance analysis of 2D & 3D microscopic image stitching techniques, microscopic ımage data set - 1 is formed by separating a series of multi-focus images into different four sub-series of multi-focus images. 2D and 3D adjacent images whose sizes are 800 x 800 x 144 are created using the sub-series of multi-focus images with auto-focusing algorithm and shape from focus strategy. Similarly, ground-truth series of multi-focus images are utilized to produce 2D and 3D ground-truth panoramic images with 1280 x 960 x 144 resolution. In order to acquire 2D multi-focus images in the ground-truth series, 10x magnification objective with 8.8 nm depth of field and 0.25 NA is used, and step motor is moved on the Z axis with 0.0125 micrometers. In order to create the series of multi-focus adjacent images in 2D microscopic ımage data set - 2, the microscope stage is moved 101 steps along the Z axis and 10 steps along the X axis. 2D and 3D adjacent images whose sizes are 1280 x 960 x 101 resolution are created using the series of multi-focus images with auto-focusing algorithm and shape from focus strategy. The number of 2D & 3D adjacent images is 10. This data set does not contain any 2D or 3D ground-truth panoramic images. In order to acquire the series of 2D multi-focus adjacent images, 20x magnification objective with 3.44 nm depth of field and 0.40 NA is utilized, step motor is moved on the Z axis with 0.0125 micrometers.

Table 1. Microscopic image data sets and properties.

Image Data Sets	Properties
Microscopic Image Data Set - 1	Number of 2D & 3D Adjacent Images = 4 3D Adjacent Image Size = 800 x 800 x 144 3D Ground-Truth Panoramic Image Size = 1280 x 960 x 144 Magnification Objective = 10x - 0.25 NA Depth of Field = 8.8 nm, Range of Step Motor = 0.0125 mm
Microscopic Image Data Set - 2	Number of 2D & 3D Adjacent Images = 10 3D Adjacent Image Size = 1280 x 960 x 101 3D Ground-Truth Panoramic Image Size = Not Icluding Magnification Objective = 20x - 0.40 NA Depth of Field = 3.44 nm, Range of Step Motor = 0.0125 mm

3.2. Performance assessment metrics

For quantitative analysis of 2D & 3D microscopic image stitching techniques, performance assessment metrics with (peak signal to noise ratio (PSNR), universal quality index (UQI), root mean square error (RMSE) and correlation coefficient (CC)) and without (kurtosis metric (KM), standard deviation (SD), entropy (EN), blur metric (BM) and average gradient (AG)) requiring a 2D or 3D ground-truth panoramic image are used. The PSNR, UQI, CC, EN, BM and AG measures of 2D or 3D panoramic image created with an ideal 2D & 3D microscopic image stitching technique are expected to be higher than other techniques. Moreover, lower RMSE, KM and SD values of the created 2D or 3D panoramic image indicate that 2D & 3D microscopic image stitching technique provides better performance than other techniques.

3.3. Quantitative and qualitative results of proposed 2D & 3D microscopic ımage stitching technique

Table 2 gives a comparison of various image stitching techniques. As mentioned in the previous sections of this study, automatic 2D or 3D microscopic image stitching is one of the most researched areas in microscopic

systems. However, there is no study in which 2D & 3D panoramic images with a wide-view sample in the microscopic system are created together as seen in Table 2. Studies that produce only a 2D panoramic image use the electron or light microscope type, while studies that produce only a 3D panoramic image use generally confocal microscope which does not need any procedure for the extraction of 3D structure and gives it automatically. Moreover, these studies do not require user input. It can be understood from Table 2 that RANSAC is the most preferred algorithm for fine registration in the studies generating only a 2D panoramic image.

Table 2. Comparison of various ımage stitching techniques.

Technique	Pano. Image Type	Micros. Type	Proc. for 3D Str.	User Input	Feature Ext. Alg.	Fine Registration	Image Fusion	Pre-processing
[1]	Only 2D	Not Mentioned	-	Semi automated	-	Least Squares	Weighted Average	-
[2]	Only 2D	Electron	-	Resize	SIFT	Cross Correlation	Linear	-
[3]	Only 2D	Light	-	No Need	Shi-Tomasi	RANSAC	Flat-Field	-
[4]	Only 2D	Light	-	No Need	SURF	RANSAC	Linear	Guaranteed Focusing
[13]	Only 2D	Light	-	No Need	SURF	RANSAC	Weighted Average	Hist. Equaliza-tion
[20]	Only 3D	Confocal	Automatic	No Need	Norm. Cross Corr.	SVD	Blenching Corr.	-
[21]	Only 3D	Confocal	Automatic	No Need	Phase Corr. and FFT	Globally Optimized Reg.	Nonlinear	-
[22]	Only 3D	Confocal	Automatic	No Need	Max. Intensity Proj.	MIP - NCC Alg.	Weighted Average	-
[29]	2D & 3D	Other Res. Fields	SFF	No Need	SURF	RANSAC	Ave. Selection	-
[30]	2D & 3D	Other Res. Fields	SFF	No Need	SURF	ICP	Ave. Selection	-
Proposed	2D & 3D	Light	SFF	No Need	SURF	Modified ICP	Ave. Selection	-

According to our literature research and as shown in Table 2, 2D & 3D panoramic images are only produced together in other research areas such as medical imaging, computer vision, remote sensing and computer graphics. Similar to these 2D & 3D image stitching techniques (2D image-based [31] and 3D image-based [30]), our proposed technique uses SFF strategy for the extraction of 3D structure. Therefore, our proposed technique cannot be compared with studies performed in other microscope types. 2D image-based [31] and 3D image-based [30] 2D & 3D image stitching techniques are only applied to our data sets in order to show the performance assessment of the proposed technique. While 2D image-based [31] and hybrid techniques

use 2D source and reference images to calculate a transformation matrix, 3D source and reference images are used in 3D image-based technique [30]. 2D image-based [31] techniques extract feature points from 2D source and reference images using the same method which is SURF. However, feature points are randomly selected from 3D source and reference images in 3D image-based technique [30]. In order to match feature points between adjacent images, 2D image-based [31], 3D image-based [30] and hybrid techniques use different methods which are Euclidean distance and K-D trees nearest neighbor search. Although 2D image-based [31], 3D image-based [30] and hybrid techniques utilize different methods which are RANSAC, Classical ICP and Modified ICP to calculate the transformation matrices in the fine registration, they use the same method, which is average selection rule to compute the pixel values and heights of overlapping areas in 2D & 3D adjacent images.

This study evaluates 2D and 3D panoramic images created with 2D image-based [31], 3D image-based [30] and hybrid techniques according to their similarities (PSNR, UQI, RMSE and CC) to 2D or 3D ground-truth panoramic images, blurring (BM), distribution (AG), randomness (EN, SD) and flatness (KM). Table 3 presents quantitative results of performance assessment metrics and execution times of 2D and 3D panoramic images created with 2D image-based [31], 3D image-based [30] and the proposed hybrid techniques on Microscopic Image Data Sets - 1 and 2. In terms of performance assessment metrics with and without requiring a 2D or 3D ground-truth panoramic image, it is clearly seen that the efficiency of the proposed hybrid technique is superior to other techniques. 3D ground-truth panoramic image, 2D and 3D panoramic images created with 2D image-based [31], 3D image-based [30] and hybrid techniques on microscopic ımage data sets - 1 and 2 are indicated in Figures 5 and 6. It is demonstrated with subjective visual results that the proposed hybrid technique produces 2D and 3D images with more clarity, less outliers and blurring.

Table 3. Quantitative results of performance assessment metrics and execution times of 2D and 3D panoramic images created with 2D image-based [31], 3D image-based [30] and hybrid 2D & 3D image stitching techniques on microscopic ımage data sets - 1 and 2.

Image Data Set	Panoramic Images	Metric	2D Image-based	3D Image-based	Hybrid
1	2D	PSNR	29.9305	30.3375	**30.4267**
		UQI	0.9864	**0.9953**	0.9912
		RMSE	5.7586	**5.4783**	5.6596
		CC	0.9976	0.9984	**0.9997**
	3D	PSNR	11.2039	15.7635	**17.7458**
		UQI	0.8140	0.9376	**0.9702**
		RMSE	12.0274	9.7536	**8.9230**
		CC	0.64874	0.8615	**0.8702**
	Execution Time (sn)		15.7432	26.8736	**9.8403**
2	2D	EN	7.0289	6.9261	**7.4670**
		BM	0.4523	**0.4612**	0.4604
		AG	115.832	120.8732	**122.2510**
	3D	KM	9.3892	6.9372	**5.4981**
		SD	56.3209	40.7640	**31.0065**
	Execution Time (sn)		38.4643	55.0643	**23.5902**

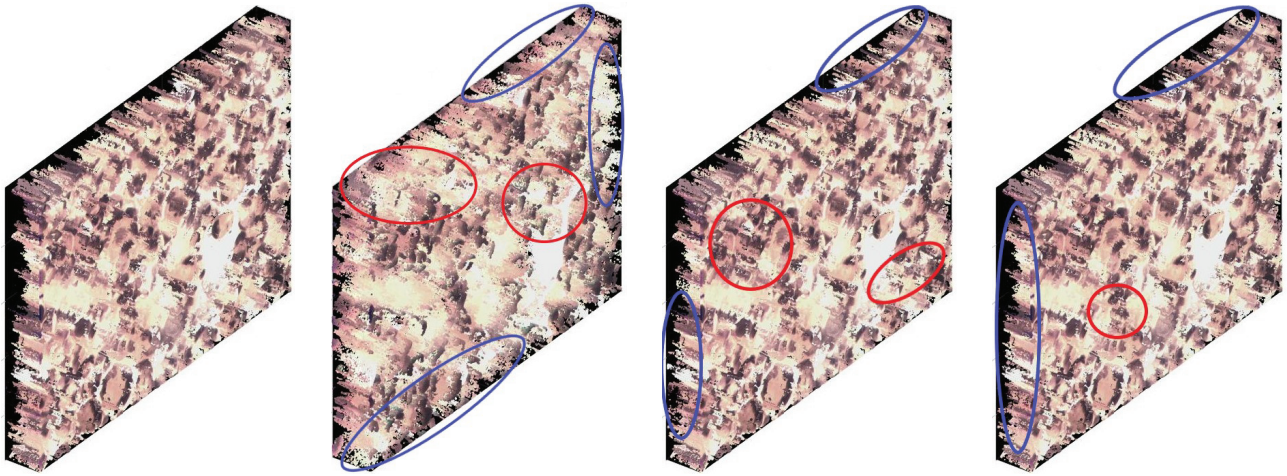

(a) (b) (c) (d)

Figure 5. 3D Ground-truth panoramic image. (a) 3D panoramic images created with 2D Image-based [31], (b) 3D Image-based [30] ,(c) Hybrid, (d) 2D & 3D image stitching techniques on microscopic image data set - 1.

4. Discussion

In this paper, a hybrid technique using modified ICP algorithm is suggested for faster and automatic 2D & 3D microscopic image stitching in cytopathologic examination. As seen in Table 2, there is no study, which creates 2D & 3D panoramic images with a wide-view of the sample in the light microscopic system together. Therefore, only 2D image-based and 3D image-based image stitching techniques, which are used in the research fields including medical imaging, computer vision, remote sensing and computer graphics can be applied to our data sets in order to show the performance assessment of the proposed technique.

The quantitative results of performance assessment metrics and execution times of 2D and 3D panoramic images created with 2D image-based [31], 3D image-based [30] and hybrid techniques on microscopic ımage data sets - 1 and 2 are given in Table 3. The values of PSNR, CC, EN and AG of 2D panoramic images created with our hybrid technique on microscopic ımage data sets - 1 and 2 are computed as 30.4267, 0.9997, 7.4670 and 122.2510. Similarly, the values of PSNR, UQI, RMSE, CC, KM and SD of 3D panoramic images created with our hybrid technique on microscopic ımage data sets - 1 and 2 are computed as 17.7458, 0.9702, 8.9230, 0.8702, 5.4981 and 31.0065, respectively. They are the best values among well-established studies for automatic 2D & 3D image stitching. According to these results, the proposed hybrid technique creates 2D and 3D panoramic images with higher similarities to 2D and 3D ground-truth images and lower blurring, distribution, randomness and flatness. From Table 3, we can see that the random selection of feature points in 3D image-based [30] technique causes computational and memory costs to increase and 2D and 3D source images to not be properly aligned to the coordinate system of 2D and 3D reference images. Instead of selecting random feature points, determining the feature points with SURF in 2D image-based [31] and proposed hybrid techniques provide the calculation of more efficient transformation matrix. Objective performance assessment metrics demonstrate that K-D trees nearest neighbor search has an essential role in faster and more accurate feature points matching between 2D and 3D adjacent images. Moreover, it is understood from quantitative results in Table 3 that the proposed hybrid technique with 9.8403 and 23.5902 (s) execution times accelerates the process of automatic 2D & 3D panoramic imaging by combining the stages of 2D image-based and 3D image-based techniques.

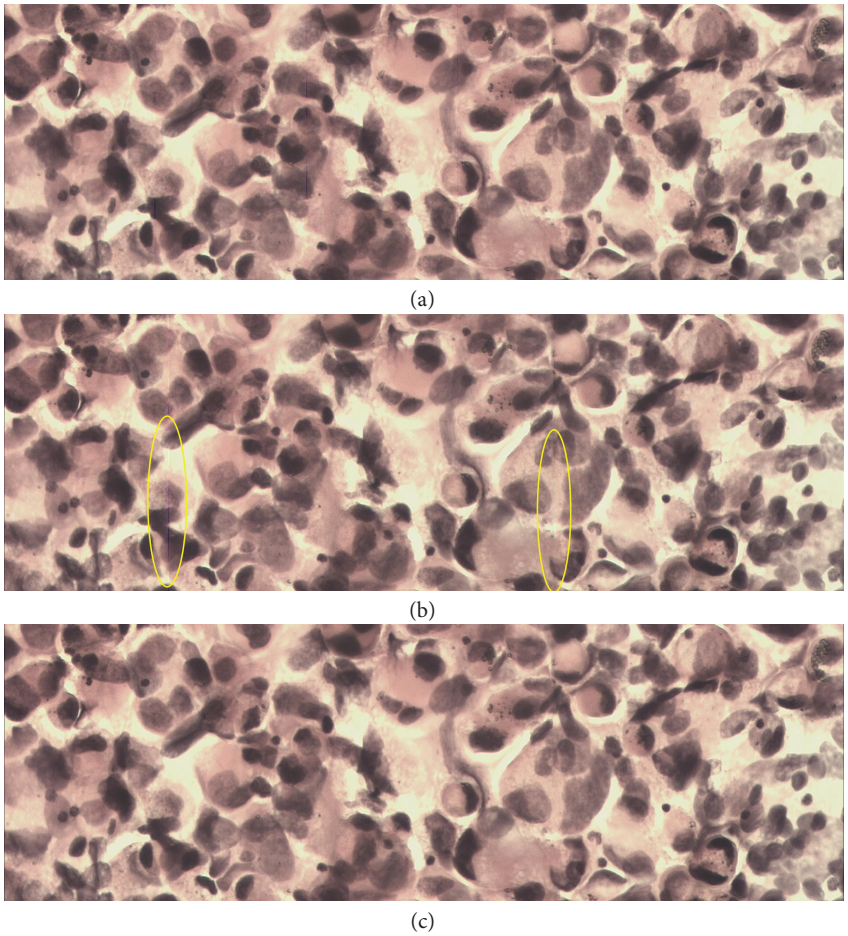

Figure 6. 2D panoramic images created with 2D Image-based [31] (a), 3D image-based [30] (b) and hybrid (c) 2D & 3D image stitching techniques on microscopic ımage data set - 2.

3D ground-truth panoramic image, 2D and 3D panoramic images created with 2D image-based [31], 3D image-based [30] and hybrid techniques on microscopic ımage data sets - 1 and 2 are indicated in Figures 5 and 6. Blue circles on Figure 5 shows that 2D image-based [31] technique produces 3D panoramic images with more outliers and artifacts. Moreover, we can understand from red circles on the Figure 5 that 3D panoramic images with less information (blur regions) are created with 2D image-based [31] technique. The reason of these restrictions (less information and more outliers) is that 2D image-based [31] technique aligns 2D and 3D source images to the coordinate system of 2D and 3D reference images using a transformation matrix (3 x 3) calculated with 2D adjacent images. As shown in Figure 5 that 3D image-based [30] technique enhances the results of 2D image-based [31] technique. However, it is seen in qualitative results in Figure 5 that 3D image-based [30] technique does not provide better 3D panoramic images than the proposed hybrid technique. Yellow circles on the Figure 6 denote that 3D image-based [31] technique creates 2D panoramic images with seams on the overlapping regions of adjacent images. The reason of these seams is that 3D image-based [30] technique selects random feature points from 3D adjacent images. Our hybrid technique prevents these shortcomings (less information, more outliers and seams on the overlapping regions) by combining the stages of 2D image-based

[31] and 3D image-based [30] techniques. It is demonstrated with subjective visual results that the proposed hybrid technique produces 2D and 3D images with more clarity, less outliers and blurring.

5. Conclusion

According to our literature research, our study is the first one in which 2D & 3D panoramic images are created together in the light microscopic system. Since it is one of the pioneering works in this field, it provides several critical advantages for cytopathologic examination. The main advantages of our study are to reduce dependence on the pathologist and to allow whole sample areas to be examined in a short time without any control (without eye-hand coordination) by providing faster and automatic 2D & 3D microscopic image stitching. Other fundamental advantages of the recommended study are explained as follows with contributions to the literature.

1. Although automatic 2D or 3D microscopic image stitching is one of the most researched areas in the microscopic systems, there is no study in which 2D & 3D panoramic images with a wide-view sample in the microscopic system are created together according to our literature research. Therefore, we think that our study, which is the first one in which 2D & 3D panoramic images with a wide-view of the sample in the microscopic system are created together, will be one of the pioneering studies in this field.

2. Contrary to 3D microscopic image stitching approaches, which are not required any 3D shape reconstruction procedure and use specific types of the microscopes (laser, stereo and confocal), our proposed technique has been developed for a light microscope system, where 2D & 3D adjacent images are created using the series of multi-focus 2D adjacent images. According to our literature research, the proposed study is the first one in which the light microscopic system is used.

3. As mentioned previously, 2D & 3D image stitching techniques are divided into two groups, 2D image-based and 3D image-based. Due to random feature points selection from 3D adjacent images in 3D image-based [30] techniques and aligning 2D and 3D source images to the coordinate system of 2D and 3D reference images using a transformation matrix (3 x 3) in 2D image-based [31] techniques, they have some limitations such as less information, more outliers and seams on overlapping regions. The second phase of this study improves a hybrid 2D & 3D microscopic image stitching technique, which combines the stages of 2D image-based and 3D image-based techniques in order to minimize their limitations. In terms of objective results obtained from the performance assessment metrics for microscope ımage data sets - 1 and 2, it is clearly seen that the efficiency of our suggested hybrid technique with the highest values of PSNR, UQI, CC, EN, BM, AG and lowest values of RMSE, KM, SD is superior to other techniques.

4. Modified ıterative closest point algorithm reduces the computational and memory costs by processing 2D adjacent images instead of 3D adjacent images (which are used in classical ıterative closest point algorithm).

5. Although modified ıterative closest point algorithm is designed for cytopathologic examination in the light microscope system, it can be adopted easily to other microscope types with different samples.

6. Realization of a novel motorized light microscope system that can provide auto-focusing and auto-scanning along the X - Y - Z axes.

Acknowledgment

This work has been supported by the TÜBİTAK Research Project 117E961.

References

[1] Thévenaz P, Unser M. User-friendly semiautomated assembly of accurate image mosaics in microscopy. Microscopy Research and Technique 2007; 70 (2): 135-146. doi: 10.1002/jemt.20393

[2] Ma B, Zimmermann T, Rohde M, Winkelbach S, He F et al. Use of autostitch for automatic stitching of microscope images. Micron 2007; 38 (5): 492-499. doi: 10.1016/j.micron.2006.07.027

[3] Piccinini F, Bevilacqua A, Lucarelli E. Automated image mosaics by non-automated light microscopes: the Micro-Mos software tool. Journal of Microscopy 2013; 252 (3): 226-250. doi: 10.1111/jmi.12084

[4] Dogan H, Ekinci M. Automatic panorama with auto-focusing based on image fusion for microscopic imaging system. Signal, Image and Video Processing 2014; 8 (1): 5-20. doi: 10.1007/s11760-014-0717-5

[5] Legesse FB, Chernavskaia O, Heuke S, Bocklitz T, Meyer T et al.. Seamless stitching of tile scan microscope images. Journal of Microscopy 2015; 258 (3): 223-232. doi: 10.1111/jmi.12236

[6] Wei L, Zhou S, Dong H, Mao Q, Lin J et al. The plant virus microscope image registration method based on mismatches removing. Micron 2016; 80: 90-95. doi: 10.1016/j.micron.2015.10.002

[7] Chernavskaia O, Guo S, Meyer T, Vogler N, Akimov D et al. Correction of mosaicking artifacts in multimodal images caused by uneven illumination. Journal of Chemometrics 2017; 31 (6): e2901. doi: 10.1002/cem.2901

[8] Seo JH, Yang S, Kang MS, Her NG, Nam DH et al. Automated stitching of microscope images of fluorescence in cells with minimal overlap. Micron 2019; 126: 102718. doi: 10.1016/j.micron.2019.102718

[9] Pang M, Chen Z, Liu S. Scale invariant feature transform gauss mosaic method for blood cell microscopic images. Journal of Medical Imaging and Health Informatics 2019; 9 (1): 134-139. doi: 10.1166/jmihi.2019.2551

[10] Ortuño JE, Lin L, del Pilar Ortega M, García-Villena J et al. Stitching methodology for whole slide low-cost robotic microscope based on a smartphone. In: 2020 IEEE 17th International Symposium on Biomedical Imaging (ISBI); Iowa City, IA, USA; 2020. pp. 503-507.

[11] Li Z, Yin Y. IC microscopic ımage stitching based on ımproved line matching. Journal of Physics: Conference Series 2020; 1607 (1): 012069. doi: 10.1088/1742-6596/1607/1/012069

[12] Hast A, Sablina VA, Sintorn IM, Kylberg G. A fast fourier based feature descriptor and a cascade nearest neighbour search with an efficient matching pipeline for mosaicing of microscopy images. Pattern Recognition and Image Analysis 2018; 28 (2): 261-272. doi: 10.1134/S1054661818020050

[13] Yang F, Deng ZS, Fan QH. A method for fast automated microscope image stitching. Micron 2013; 48: 17-25. doi: 10.1016/j.micron.2013.01.006

[14] Lu Y, Gao Q, Chen S, Sun D, Xia Y et al. Fast implementation of image mosaicing on gpu. In: 2017 10th International Congress on Image and Signal Processing, BioMedical Engineering and Informatics (CISP-BMEI); Shanghai, China; 2017. pp. 1-5.

[15] Ma B, Ban X, Huang H, Liu W, Liu C et al. A fast algorithm for material image sequential stitching. Computational Materials Science 2019; 158: 1-13. doi: 10.1016/j.commatsci.2018.10.044

[16] Baik JW, Kim JY, Cho S, Choi S, Kim J et al. Super wide-field photoacoustic microscopy of animals and humans in vivo. IEEE Transactions on Medical Imaging 2019; 39 (4): 975-984. doi: 10.1109/TMI.2019.2938518

[17] Voleti V, Patel KB, Li W, Campos CP, Bharadwaj S et al. Real-time volumetric microscopy of in vivo dynamics and large-scale samples with scape 2.0. Nature methods 2019; 16 (10): 1054-1062. doi: 10.1038/s41592-019-0579-4

[18] Gurkan G, Gurkan K. Incu-Stream 1.0: An open-hardware live-cell ımaging system based on ınverted bright-field microscopy and automated mechanical scanning for real-time and long-term ımaging of microplates in ıncubator. IEEE Access 2019; 7: 58764-58779. doi: 10.1109/ACCESS.2019.2914958

[19] Bowditch E, Kadonosono K, Chang A. Heads-up microscope systems in vitreoretinal surgery. Macular Surgery 2020; 179-188. doi: 10.1007/978-981-15-7644-7_13

[20] Emmenlauer M, Ronneberger O, Ponti A, Schwarb P et al. XuvTools: free, fast and reliable stitching of large 3D datasets. Journal of Microscopy 2009; 233 (1): 42-60. doi: 10.1111/j.1365-2818.2008.03094.x

[21] Preibisch S, Saalfeld S, Tomancak P. Globally optimal stitching of tiled 3D microscopic image acquisitions. Bioinformatics 2009; 25 (11): 1463-1465. doi: 10.1093/bioinformatics/btp184

[22] Bria A, Iannello G. TeraStitcher a tool for fast automatic 3D stitching of teravoxel-sized microscopy images. BMC Bioinformatics 2012; 13 (1): 1-15. doi: 10.1186/1471-2105-13-316

[23] Chalfoun J, Majurski M, Blattner T, Keyrouz W, Bajcsy P et al. Mist: accurate and scalable microscopy image stitching tool with stage modeling and error minimization. Scientific Reports 2017; 7 (1): 1-10. doi: 10.1038/s41598-017-04567-y

[24] Millis BA, Tyska MJ. High-resolution image stitching as a tool to assess tissue-level protein distribution and localization. Molecular Profiling 2017; 1606: 281-296. doi: 10.1007/978-1-4939-6990-6_18

[25] Ye W, Yu K, Yu Y, Li J. Logical stitching: A panoramic image stitching method based on color calibration box. In: 2018 14th IEEE International Conference on Signal Processing (ICSP); Beijing, China; 2018. pp. 1139-1143.

[26] Horl D, Rusak FR, Preusser F et al. Bigstitcher: reconstructing high-resolution image datasets of cleared and expanded samples. Nature Methods 2019; 16 (9): 870-874. doi: 10.1038/s41592-019-0501-0

[27] Berman A, Quek F. ThingiPano: a large-scale dataset of 3d printing metadata, ımages, and panoramic renderings for exploring design reuse. In: 2020 IEEE Sixth International Conference on Multimedia Big Data (BigMM); New Delhi, India; 2020. pp. 18-27.

[28] Yanny K, Antipa N, Liberti W et al. Miniscope3D: optimized single-shot miniature 3D fluorescence microscopy. Light: Science Applications 2020; 9 (1): 1-13. doi: 10.1038/s41377-020-00403-7

[29] Gledhill D, Tian GY, Taylor D, Clarke D. Panoramic imaging — a review. Computers & Graphics 2003; 27 (3): 435-445. doi:10.1016/S0097-8493(03)00038-4

[30] Chen Y, Medioni G. Object modelling by registration of multiple range images. Image and Vision Computing 1992; 10 (3): 145-155. doi: 10.1016/0262-8856(92)90066-C

[31] Dogan H, Baykal E, Ercin ME, Ersoz S, Ekinci M. A novel 2d and 3d wide-view imaging approach by controlling optimal range for cytopathological analysis in light microscopic system. Optics Communications 2019; 430: 39-50. doi: 10.1016/j.optcom.2018.08.032